Portfolio Decision Analysis for Risk-Based Maintenance of Gas Networks

Tommaso Sacco[a], Michele Compare[b,c], Enrico Zio[b,c,d,e], Giovanni Sansavini[a]

[a] *Risk and Reliability Engineering Laboratory, ETH Zürich, Switzerland*
[b] *Energy Department, Politecnico di Milano, Italy*
[c] *Aramis Srl, Milano, Italy*
[d] *Chair on Systems Science and Energetic Challenge, Fondation EDF (Electricite' de France) CentraleSupelec, Universite' Paris-Saclay, France*
[e] *Eminent Scholar, Department of Nuclear Engineering, College of Engineering, Kyung Hee University, Republic of Korea*

Abstract

Maintenance is fundamental for the safe and profitable operation of many critical assets, including gas networks. The inherent complexity of these assets and budgetary constraints pose significant challenges to the decision-making related to maintenance management, which requires trading-off among conflicting objectives while respecting technical and normative constraints. The difficulty of such decision-making is due to incomplete knowledge about the technical parameters, operating conditions and degradation states of the components. We address the challenge by proposing a risk-based maintenance framework for supporting decision makers in selecting maintenance plans that are optimal with respect to the objectives and constraints considered. We apply Robust Portfolio Modeling (RPM) to identify those maintenance decisions that are most effective for reducing the severity and likelihood of failures in the gas network. RPM allows us to handle partial knowledge on the objective values and on the preferences of decision-makers. We lay down the complete steps of the framework, including the quantification of the likelihood of failures and their consequences for the population and for the gas network operation. The framework is demon-

Email addresses: tommaso.sacco@mail.com (Tommaso Sacco), michele.compare@polimi.it (Michele Compare), enrico.zio@polimi.it (Enrico Zio), sansavig@ethz.ch (Giovanni Sansavini)

strated on the high pressure natural gas pipeline network of Great Britain. The results reveal that if there are no constraints on the budget, maintenance actions are focused on some critical zones, e.g. Scotland and the southernmost part of England. Instead, if fixed maintenance budgets are allocated to different areas, the maintenance projects selected are sub-optima and a smaller risk reduction is achieved over the maintenance horizon.
Keywords: Maintenance, Natural Gas Networks, Robust Portfolio Modeling, Failure Likelihood and Severity

1. Introduction

High-pressure Natural Gas Networks (NGNs) are complex systems that transfer natural gas to off-takes spread over vast areas and provide a primary resource to produce electricity. Failures in the pipelines that transport the flammable natural gas can compromise the network stability and cause accidents with significant damages to the surrounding environment and population. In practice, maintenance budgets are such that they require prioritization of the maintenance interventions on the different portions of the infrastructure.

To address the problem of maintenance budget allocation, decision makers (DMs) can rely on Multi-Criteria Decision Making (MCDMs) models. For instance, Marsaro et al. propose a framework to minimize the impact of accidents in natural-gas pipeline networks, with respect to human, financial and environmental consequences [1]. Candian et al., apply the Analytic Hierarchy Process (AHP, [2]) for the prioritization and selection of maintenance plans from a portfolio of possible ones ([3]). Pilavachi et al., use MCDM models to select the least risky technologies among different alternatives for building natural gas and hydrogen-fired power plants [4]. MCDM models have been applied for pipeline risk assessment by Jamshidi et al. ([5]), where the relative risk score methodology ([6, 7]) and fuzzy logic ([8]) are integrated to treat imprecise information. In Dey et al. ([9]), the Analytic Hierarchy Process is used to characterize risk and allocate maintenance budget. The optimal operating conditions of a nat-

ural gas network are identified in ([10]) via a multi-objective genetic algorithm considering three conflicting objectives, i.e. gas delivery flow and line pack, to be maximized, and operating cost, to be minimized.

Despite the successful application to literature case studies, MCDM models find limited use in real gas network contexts, because they are unable to address some practical problems, i.e.,

- handle the incomplete knowledge of the parameters influencing network operations and, thus, the values of the projects with respect to the objectives;
- accommodate the imprecision in the decision maker's preference statements about the importance of the decision objectives;
- consider synergies among the projects and other mutual inter-dependencies or constraints (e.g., the minimum amount of projects per area);
- use optimization algorithms capable of identifying non-dominated project portfolios from a large (i.e., a few thousands) set of candidate alternatives.

The aforementioned issues can be effectively addressed by the Robust Portfolio Modeling (RPM) technique ([11, 12]), which has been successfully applied in [13] to select cost-effective portfolios (i.e., sets) of projects in support to maintenance budget allocation for transportation networks. Moreover, the non-deterministic optimization algorithm used therein can identify the subsets of the portfolio Pareto set, in acceptable computational times [13]. RPM has also been applied in [14] for maintenance budget allocation in sewerage networks, where a Risk-Based Maintenance (RBM) approach has been embraced ([9, 15]). There, the maintenance allocation issue is framed as a two-objective decision problem, considering risk and cost: the larger the reduction in the overall asset risk yielded by maintaining a given network item, the higher the priority of the maintenance project. By embedding the RBM approach within RPM, resources can be cost-effectively allocated to provide a high priority to high-risk items, while still guaranteeing the adequate effort on low-risk items.

Building on [14], RPM has been investigated in [16] in support to RBM of pipelines for a scaled-down model of the National Grid (NG) high-pressure NGN. This preliminary work makes several simplifying assumptions, which are overcome in the present work, in an effort to build a full-fledged methodology in support to maintenance decision making in real gas network maintenance management problems.

In this paper, we propose a risk-based maintenance framework to support decision makers in the selection of optimal maintenance plans. The framework applies RPM to identify those maintenance actions which can most reduce the severity and likelihood of failures in the gas network. The framework includes the quantification of failure probabilities and of failure consequences for the surrounding population and the operation of the gas network. In details, the following advancements are introduced: (*i*) both risk factors (i.e., failure likelihood and failure severity) are thoroughly characterized through the identification and characterization of their relevant sub-factors (e.g., external corrosion, third party actions for failure probability); (*ii*) Geographic Information System (GIS) data are used to estimate the values of the maintenance plans with respect to some of the identified risk sub-factors; (*iii*) sequential portfolio selection is considered on an horizon of multiple years, and with different objectives and constraints: this allows investigating how the network risk changes over time, and correspondingly the maintenance allocation.

The remainder of the paper is organized as follows. Section 2 introduces RBM and RPM. Section 3 describes the risk assessment methodology for NGNs and details the procedure to estimate the failure probability for the different failure modes of the pipelines. Section 4 illustrates the approach for the estimation of the failure severity. Section 5 presents the quantification of failure severity and failure probability. Section 6 shows a practical application of the framework to the case study of the NGN of Great Britain. Section 7 outlines some considerations about the applicability of the methodolgy to other contexts. Finally, Section 8 concludes the paper.

2. Risk-based maintenance of large NGNs

In the RBM framework for NGN maintenance, the risk of failure, R, is considered as the driving criteria to allocate maintenance efforts on the network. The factors characterizing risk are: likelihood of the occurrence of the failure event and severity of the impact of the failure on people, properties, environment, safety, production, etc.

To identify the gas network elements impacting most on these two risk factors, we build on [9], [15] and [16], and propose a framework for selecting the relevant risk sub-factors and estimating their values in the alternative maintenance projects. Due to incomplete knowledge on the network technical and operational parameters, these values are affected by uncertainties, here represented as intervals of possible values.

In this study, the maintenance action performed on a pipeline corresponds to its replacement, which reduces the failure probability by removing the effects of aging and degradation. The cost of a maintenance action depends on the length of the replaced pipeline segment. Costs are imprecisely known and their estimates are also provided as intervals of possible values.

RPM is applied to identify the portfolios of pipeline segments which have the largest impact on reducing risk at the smallest maintenance costs. Details of the RPM approach are provided in Appendix A.

3. Pipeline Failure Probability

According to [17], the pipeline failure probability mainly depends on external corrosion, internal corrosion and third party actions. In this Section, we outline a procedure to quantify the contributions of these sub-factors to the failure likelihood.

3.1. External Corrosion

External corrosion is caused by the propagation of corrosion defects along the pipeline wall thickness, which can ultimately lead to gas leakage, burst or asset

disruption [18]. In this study, we focus on the localized corrosion phenomena, which result in faster defect growth as compared to generalized corrosion, and, consequently, pose more severe threats to pipeline asset integrity [19].

Empirical studies show that the localized defects growth is well represented by a lower-than-one power law trend [18, 20]. Accordingly, the most broadly-accepted model is the one introduced by [21], which reads

$$d_{max}(t) = k(t - t_0)^a \tag{1}$$

where $d_{max}(t)$ is the maximum external defect depth at time t, whereas t_0 is the corrosion starting time. Coefficients k and a can be estimated through the following weighted sums of parameters related to the properties of the soil, where the pipe is buried [22, 23]

$$\begin{aligned} k &= k_0 + k_1 \times rp + k_2 \times pH + k_3 \times re + k_4 \times cc + k_5 \times bc + k_6 \times sc \\ a &= a_0 + a_1 \times pp + a_2 \times wc + a_3 \times bd + a_4 \times ct \end{aligned} \tag{2}$$

where rp is the soil red-ox potential in mV; pH is the soil pH; re is the soil resistivity in $\Omega \times m$; cc, bc and sc are the chloride, bicarbonate and sulphate contents of the soil, respectively, measured in ppm. Table 1 shows for different soil types, the probability distributions with corresponding parameters describing the uncertainty in these values [22, 24].

Coefficients $k_0, ..., k_6$ depend on the properties of the soil (Table 2).

The empirical relationship for coefficient a in Equation 2 contains pp, i.e. the pipe-to-soil potential measured in mV, wc, i.e. the percentage water content, bd, i.e. the soil bulk density in g/mL. These parameters are described by the probability distributions in Table 1.

Empirical coefficients $a_0, ..., a_4$ are reported in Table 2 ([22, 24]). Finally, ct is a scoring factor related to the pipe coating type and soil type (Table 3).

The failure probability by external corrosion at time t, $P_E(t)$, is estimated by checking the corrosion depth against three failure thresholds g_1, g_2 and g_3 [25], which correspond to the safety limits for small leakage, burst and rupture, respectively. These threshold values are defined as

Table 1: Soil properties and corresponding probability distributions [22, 24]. Mean and variance are reported in brackets.

Variable, Symbol (units)	Probability Density Function			
	Clay	Clay Loam	Sandy Clay Loam	Other
Resistivity, re (Ω-m)	Weibull (62, 4275)	Weibull (28,566)	Lognormal (49, 2363)	Lognormal (50,2931)
Sulphate, sc (ppm)	Gamma (131, 12566)	Lognormal (208, 65549)	Weibull (144, 9836)	Lognormal (154, 25328)
Bicarbonate, bc (ppm)	Lognormal (19,639)	Lognormal (23, 548)	Lognormal (14, 36)	Lognormal (19, 436)
Chloride, cc (ppm)	Lognormal (53, 4709)	Lognormal (45, 2946)	Lognormal (22, 559)	Lognormal (41, 3135)
Watercontent, wc (%)	Normal (24, 47)	Weibull (25, 27)	Normal (22, 33)	Normal (24, 38)
pH, pH	Gumbel (5.94, 0.97)	Gumbel (6.36, 0.77)	Normal (6.23, 0.637)	Gumbel (6.13, 0.84))
Pipe/Soil potential, pp (V)	Normal (-0.86, 0.04)	Normal (-0.81, 0.04)	Normal (0.92, 0.023)	Normal (-0.86, 0.04)
Bulk density, bd (g/ml)	Normal (1.22, 0.003)	Gumbel (1.32, 0.0005)	Gumbel (1.39, 0.002)	Normal (1.30, 0.007)
Redox Potential, rp (mV)	Uniform (2.14, 348)	Uniform (19, 301)	Uniform (20, 339)	Uniform (2.14, 348)

Table 2: Coefficients of Equations 1 and 2 for the four types of soil analyzed in this study [22, 24].

Parameter (variable, symbol)	Clay	Clay Loam	Sandy Clay Loam	Other
k_0	5.51E-01	9.84E-01	5.59E-01	6.08E-01
a_0	8.85E-01	2.82E-01	9.65E-01	8.96E-01
t_0 (years)	3.05	3.06	2.57	2.88
k_1 (redox potential, rp)	-8.98E-05	-1.06E-04	-1.82E-04	-1.80E-04
k_2 (pH, pH)	-5.90E-02	-1.15E-01	-6.42E-02	-6.54E-02
k_3 (resistivity, re)	-2.15E-04	-2.99E-04	-2.12E-04	-2.60E-04
k_4 (chloride, cc)	8.38E-04	1.80E-03	8.62E-04	8.74E-04
k_5 (bicarbonated, bc)	-1.28E-03	-4.88E-04	-6.78E-04	-6.39E-04
k_6 (sulphate, sc)	-5.33E-05	-2.09E-04	-1.13E-04	-1.22E-04
a_1 (pipe/soil potential, pp)	4.93E-01	4.61E-01	5.12E-01	5.19E-01
a_2 (water content, wc)	3.72E-03	1.69E-02	4.50E-04	4.65E-04
a_3 (bulk density, bd)	-1.01E-01	-9.87E-02	-1.58E-01	-9.90E-02
a_4 (coating type, ct)	4.67E-01	5.67E-01	4.34E-01	4.31E-01

Table 3: Scoring factors, *ct*, and coating type frequency by soil category for the four types of soil examined in this study [22, 24].

Coating type	Score
Bare pipe	1
Asphalt Enamel	0.9
Wrap Tape	0.8
Coal Tar	0.7
FBE	0.3

$$g_1 = 0.8th - d_{max}(t) \tag{3}$$

$$g_2 = r_b(t) - p \tag{4}$$

$$g_3 = r_{rp} - p \tag{5}$$

where th is the pipeline wall thickness; p is the pipeline internal pressure; r_b and r_{rp} are the burst and the rupture pressure, respectively. Details on the threshold models are reported in Appendix B.

The following Monte Carlo (MC) simulation procedure has been applied for propagating the epistemic uncertainties on the model parameters related to the soil type [25] (Table 1) onto the reliability of each pipeline segment:

1. Once the type of soil in which the pipeline is buried is identified, the parameters related to its properties are sampled from the corresponding distributions in Table 1 to estimate parameters k and a (Eq. 2).
2. The propagation of the defect depth in the pipeline wall is simulated through yearly time steps. The pipeline failure is detected by comparison of the defect depth with the three thresholds g_1, g_2 and g_3. In detail, the following decision logic is applied [25]:
   (a) Small leakage occurs if $g_1 \leq 0$ and $g_2 \geq 0$. This result is not affected from the value of g_3.
   (b) Large leakage occurs if $g_1 > 0$, $g_2 \leq 0$ and $g_3 > 0$.
   (c) Rupture occurs if $g_1 > 0$, $g_2 \leq 0$ and $g_3 \leq 0$.

   The pipelines fail in all other possible situations.
3. The year in which the failure occurs is recorded and the MC simulation proceeds to the next iteration.
4. For every time t, the portion of failed pipelines is registered, together with the 80% confidence interval on the MC estimates.

3.2. Internal Corrosion

Internal corrosion is considered as one of the main causes of pipeline failure [23]. To quantify its contribution, P_I, to failure probability, the approaches

based on numerical simulations cannot be adopted, due to their computational burden for large NGNs.

Therefore, the defect growth by internal corrosion is modeled as a function of natural gas properties ([26])

$$\begin{aligned}\frac{d\alpha}{dt} = \kappa \times C_I \times 0.0254 \times (8.7 + 9.86 \times 10^{-3} O_2 - 1.48 \times 10^{-7} O_2^2 \\ - 1.31 pH + 4.93 \times 10^{-2} \phi_{CO_2} \phi_{H_2S} \\ - 4.82 \times 10^{-5} \phi_{CO_2}\ O_2 - 2.37 \times 10^{-3} \phi_{H_2S}\ O_2 \\ - 1.11 \times 10^{-3} O_2\ pH)\end{aligned} \tag{6}$$

where α is the internal defect length (in mm), t is the time (years), κ is the multiplicative factor related to the corrosion model error, O_2 is the oxygen concentration, in ppm, ϕ_z is the partial pressure of compound $z \in \{H_2S, CO_2\}$ in the transported gas, pH is, again, the pH of the substance and, finally, C_I is the inhibitor correction factor, which takes into account the introduction of corrosion preventing agents typically injected into the pipelines for protection. Specifically, C_I is defined as

$$C_I = 1 - e^{(-A \frac{L}{L_0})} \tag{7}$$

where, according to [26], A is a multiplication factor obeying a log-normal distribution with mean -0.1116 and standard deviation 0.4724, $L_0 = 5Km$ is the characteristic length of the inhibitor effects, and L is the distance from the injection point where the pitting corrosion defect nucleates. This follows a uniform probability distribution in $[0, L_0]$.

The parameters of the internal-corrosion model related to the natural gas properties are affected by epistemic uncertainty, which is described by the probability distributions reported in Table 4 ([26]). The failure probability for internal corrosion over time, $P_I(t)$, can be estimated through the Monte Carlo procedure used for external corrosion (Section 3.1), where the pipeline failure is identified by comparing the defect depth to the same failure thresholds g_1, g_2 and g_3 [25, 26].

Table 4: Natural gas properties distributions originally reported in [26].

Random Variable (units)	Distribution Type	Mean	Standard Deviation
T (degree K)	Normal	289	28.9
% CO_2 (mole)	Lognormal	5	1
O_2 (ppm)	Lognormal	5000	1500
pH	Lognormal	6	1
% H_2S (mole)	Lognormal	0.05	0.005
P (Pascal)	Lognormal	408000	808000
k, corrosion model error	Lognormal	1	0.5
A, inhibitor factor	Lognormal	1	0.5

3.3. Third Party Action

The importance of third party actions in determining the failure probability depends on a large spectrum of circumstances related to the activities of third parties in the proximity of the pipeline. Some authors adopted fault tree analysis to estimate the probability of failure due to third party activities [27, 28]. Nevertheless, the deep level of detail these models require is not compatible with the need of making decisions on a large-size network in the presence of incomplete information.

According to [29], we assume that the failure probability by third party actions, P_{TP}, follows the constant hazard rate model, i.e. $P_{TP} \sim exp(\lambda_{TP})$, where λ_{TP} reads

$$\lambda_{TP} = \lambda(D)\ a_c\ a_w\ a_l\ a_p \tag{8}$$

in which $\lambda(D)$ is the baseline failure frequency due to third party actions for a pipeline of diameter D [29], whereas the following multiplication coefficients are related to the buried pipeline property: wall thickness a_w, location a_l, depth of cover a_x and installed preventive measures a_p. Table 5 provides the values of the multiplication coefficients estimated in [29].

In this study, the pipeline diameter and the location are precisely known, while the remaining two parameters are conservatively assumed as the largest values of

Table 5 (i.e. 3.3 and 1 for the depth of cover and installed preventing measures, respectively).

Table 5: Coefficients of the model for failure due to third party actions developed in [29].

Parameter	Coefficient	Categories	Value
wall thickness	a_w	Minimal design thickness	1
		Above minimal design thickness	0.2 - 0.4
location	a_l	Rural	1
		Suburban	3.9
		Urban	23.1
depth of cover	a_c	< 0.91 m	3.3
		0.91- 1.22 m	1
		>1.22 m	0.7
installed preventing measures	a_p	Marker Posts	1
		All other prevention measures	0.9

4. Failure Severity

Failure severity is considered to depend on two factors, i.e. (i) consequences to people and (ii) consequences on the stability of the network operations. The characterization of these factors is detailed in Sections 4.1 and 4.2, respectively.

4.1. Consequences to People

Due to the large amount of gas transported in the pipelines, their failure may lead to large releases of flammable substances jeopardizing widespread areas in the surrounding.

Based on [30], we consider three main fire phenomena due to pipeline failure: jet-fire, jf, fireball, fb, and flash fire, ff. For each of them and for each pipeline segment $i \in X$, we identify, through the *Buffer* geo-processing tool in ArcMap, the hazard distance δ_j^i, $j \in \{jf, fb, ff\}$ and the corresponding hazard area (i.e., the area located within a distance equal to or smaller than δ_j^i from the pipeline). Then, the population insisting on the hazard area is estimated by identifying the type of area category $LC \in \{rural, urban, suburban\}$, whose upper and lower bounds of the standard population densities, $\overline{pd_{LC}}$ and $\underline{pd_{LC}}$, respectively, are

Table 6: Fire phenomenon probability given a pipeline failure [30, 32].

Fire phenomenon	Probability
Jet Fire (*jf*)	0.3
Fire Ball (*fb*)	0.3
Flash Fire (*ff*)	0.504

Table 7: Standard population densities used in safety assessments [31].

Population Density [km^{-2}]		
Area	Upper Bound	Lower Bound
Rural	1	0
Suburban	40	5
Urban	120	40

available in [31]. These values are reported in Table 7.

Finally, the upper and lower bounds, $\overline{\Sigma}_i$ and $\underline{\Sigma}_i$, respectively, of the severity of the consequences for people from the failure of pipeline $i \in X$ buried in location category LC, are estimated as

$$\begin{aligned} \underline{\Sigma}_i &= \min_{j \in \{jf, fb, ff\}} \underline{\xi}_j^i \\ \overline{\Sigma}_i &= \max_{j \in \{jf, fb, ff\}} \overline{\xi}_j^i \end{aligned} \tag{9}$$

where $\underline{\xi}_j^i = \delta_j^i \times l^i \times \underline{pd_{LC}}$ and $\overline{\xi}_j^i = \delta_j^i \times l^i \times \overline{pd_{LC}}$ represent the lower and upper bounds, respectively, of the number of people affected by each of the three fire phenomena, being l^i the length of pipe $i \in X$. The three phenomena are considered independent on each other. The values of the weights are taken from [30, 32] and are reported in Table 6.

Jet-fire. Hazard distances for jet-fire are estimated according to the empirical formula proposed in [33]

$$\delta_{jf} = 19.50 \; Q^{0.447} \tag{10}$$

where Q is the flammable gas release rate in kg/m^2, assumed equal to the natural gas mass flowing in the pipe [34, 35].

Fire-ball. The hazard distance for a fireball phenomenon is estimated using the empirical formula proposed in [33, 36]

$$P_R(x) = P_S \cdot F(x)\gamma T \tag{11}$$

which links the received heat flux $P_R(x)$ at a distance x from the point directly under the fireball to the surface power density, P_S, the view factor, $F(x)$ (i.e., a parameter related to the fraction of heat received by the receptor body), the absorptivity of the receptor body, γ, and the atmospheric transmissivity T. In details,

$$P_S = \frac{\phi M H_c}{\pi (D_{max})^2 t_{fb}} \tag{12}$$

where $\phi = 0.3$ is the radiation fraction, M is the mass of flammable material, as calculated by the mass flow model, $H_c = 50\ kJ/g$ is the heat of combustion of natural gas, $D_{max} = 6.48M^{0.325}$ is the maximum fireball diameter, $t_{fb} = 0.825M^{0,26}$ is the fireball duration time. According to [33, 36], the view factor in Eq. 11 is estimated as

$$F = \frac{D_{max}^2}{4(x^2 + H^2)} \tag{13}$$

where H is the elevation fireball, estimated as $H = 0.75D_{max}$. Finally, the atmospheric transmissivity is defined as

$$T = 1.30/(p_w R_T)^{0.09} \tag{14}$$

where p_w is the partial pressure of water, hereby assumed as 0.6105, while $R_T = (x^2 + H^2)^{0.5} - 0.5D_{max}$ is the distance of the receiver from the fireball

external border.

The hazard distance is defined as

$$\delta_{fb} = min\{x \in \Re | P_R(x) < 5.0\ kW/m^2\} \tag{15}$$

This is numerically estimated by solving Eq. 11 as a function of the distance x.

Flash Fire. Flash fire is modeled as the well-known Gaussian plume model [37]. Namely, the density of the gas is distributed as a Gaussian from an instantaneous point release source [33]. The hazard distance for flash fire δ_{ff} is defined as the point at which the natural gas concentration drops below the lower flammability limit, hereby assumed as 5.0% in volume-volume of air [32, 30]. The distance is calculated using the Matlab Guassian Plume model ([38]), conservatively assuming wind speed equal to 10 m/s and gas release from ground level.

4.2. Consequences on Network Stability

Large pipeline networks are generally equipped with several redundancies and safety mechanisms for preventing failures to cause severe instabilities. Nonetheless, some network elements remain fundamental for the stability of network operations, because their failures may isolate off-takes or large gas terminals and cause pressure instabilities that can be compensated only by curtailing the gas load.

The gas flow in the network is modeled according to [35], which applies Kirchoff law of networks and computes the pressure at every node of the gas network [34, 35]. In formulas, this entails that

$$\sum_{i=1}^{m_k} b_{ki} \Delta\varphi_i = 0 \quad k = 1, ..., K \tag{16}$$

where m_k is the number of pipelines in loop k, K is the number of closed loops in the network, b_{ki} defines the sign of the pressure difference in pipe $i \in X$ of loop k and $\Delta\varphi_i$ is the pressure drop across pipeline i. Although the removal of a pipeline in the network is a local phenomenon, it has the potential to cause violations of the pressure safety limits in the gas transmission across the

network. Thus, the loss or the removal of pipelines from the network topology has a global impact ([34, 35]).

Specifically, to assess whether the failure of a pipeline causes instability, we remove it from the network structure and solve Eq. 16 to compute the updated steady-state flow conditions. These are constrained to the safety requirements on maximum and minimum pressures in the pipelines. Possible safety pressure violations, therefore, are mitigated (i) by adjusting the intake of gas from supply terminals and storages, and, (ii) by curtailing some of the gas demand located close to the pressure violation areas, if the former actions are not sufficient. If the system cannot satisfy the entire gas demand following the loss of pipeline $i \in X$ because of off-takes disconnections or curtailments required to reach safe steady-state conditions [34], the amount of gas demand not served, DNS_i, is used as the indicator of the severity for network stability.

5. Pipeline Failure Risk

Following the quantification of the pipeline failure probabilities for the three failure modes detailed in Section 3 and the quantification of the severity of their consequences to people and NGN operations detailed in Section 4, the failure likelihood and severity for each pipeline segment $i \in X$ are estimated.

Likelihood. The lower and upper bounds of the failure probability of pipeline section $i \in X$, $\underline{\mathcal{P}}_i$ and $\overline{\mathcal{P}}_i$, respectively, are estimated by combining the corresponding lower ($\underline{P_{I}}_i, \underline{P_{E}}_i, \underline{P_{TP}}_i$) and upper ($\overline{P_{I}}_i, \overline{P_{E}}_i, \overline{P_{TP}}_i$) bounds of the failure probabilities of the three failure modes. These are assumed to be statistically independent and the rare event approximation is used for their combination [39], whereby we can write

$$\begin{aligned} \underline{\mathcal{P}}_i &= \underline{P_{I}}_i + \underline{P_{E}}_i + \underline{P_{TP}}_i \\ \overline{\mathcal{P}}_i &= \overline{P_{I}}_i + \overline{P_{E}}_i + \overline{P_{TP}}_i \end{aligned} \tag{17}$$

Whilst the independence of failure by third party actions on corrosion is evident, that of internal and external corrosion deserves a justification. As

mentioned before, the generalized corrosion phenomenon is here neglected to focus on localized phenomena [19, 24]. The localized corrosion impacts on a very small area of the pipeline surface, whereby the probability that two localized phenomena occur in the same location is negligible.

For a consistent comparison of failure likelihood and severity, the failure probabilities of the pipeline segments are normalized in the [0,1] interval to give the values of the failure likelihood. These are given by

$$\begin{aligned} \underline{\mathcal{L}}_i &= \frac{\underline{\mathcal{P}}_i - \underline{\mathcal{P}}_{min}}{\overline{\mathcal{P}}_{max} - \underline{\mathcal{P}}_{min}} \\ \overline{\mathcal{L}}_i &= \frac{\underline{\mathcal{P}}_i - \overline{\mathcal{P}}_{min}}{\overline{\mathcal{P}}_{max} - \underline{\mathcal{P}}_{min}} \end{aligned} \tag{18}$$

where $\overline{\mathcal{P}}_{max} = \max_{i \in X} \overline{\mathcal{P}}_i$ and $\underline{\mathcal{P}}_{min} = \min_{i \in X} \underline{\mathcal{P}}_i$

Severity. To take into account the consequences to both people and to NGN operations stemming from the failure of pipeline segment $i \in X$, the lower and upper bounds of the corresponding severity scores are lumped together via the following formulas

$$\begin{aligned} \overline{S}_i &= 0.95\ \overline{\mathcal{S}}_i + 0.05\ \mathcal{DNS}_i \\ \underline{S}_i &= 0.95\ \underline{\mathcal{S}}_i + 0.05\ \mathcal{DNS}_i \end{aligned} \tag{19}$$

where

$$\begin{aligned} \underline{\mathcal{S}}_i &= \frac{\underline{\Sigma}_i - \underline{\mathcal{S}}_{min}}{\overline{\mathcal{S}}_{max} - \underline{\mathcal{S}}_{min}} \\ \overline{\mathcal{S}}_i &= \frac{\overline{\Sigma}_i - \underline{\mathcal{S}}_{min}}{\overline{\mathcal{S}}_{max} - \underline{\mathcal{S}}_{min}} \end{aligned} \tag{20}$$

where $\overline{\mathcal{S}}_{max} = max_{i \in X} \overline{\Sigma}_i$ and $\underline{\mathcal{S}}_{min} = min_{i \in X} \underline{\Sigma}_i$. The same normalization procedure is applied to $\mathcal{DNS}_i$.

This weighted-sum approach allows integrating the severity factors, attributing a higher importance to the consequence to people (through a weight equal to 0.95) than to the consequences on network stability (weight equal to 0.05).

Cost. Each maintenance activity is associated to a cost. Following a common practical approach, we take the cost of replacing pipeline segment $i \in X$ as that of a brand new pipeline segment; this cost is proportional to a base cost c, the pipeline diameter D_i and the pipeline length l_i [40, 41]. To give account to the uncertainties associated with the time and spatial scales of the maintenance actions, we assume that the specific maintenance cost can range between $\underline{c}$ and $\overline{c}$

$$\begin{aligned} \overline{C}_i &= \overline{c} \times D_i \times l_i \\ \underline{C}_i &= \underline{c} \times D_i \times l_i \end{aligned} \tag{21}$$

This approach is consistent with the representation of the uncertainty for failure likelihoods and severities, which are also described by intervals of possible values.

6. Case Study: High Pressure Gas Transmission Network of Great Britain

6.1. Structural properties

The risk-based portfolio selection methodology is illustrated via a case study on the British National Grid high pressure NGN, containing 7660 km of pipelines and delivering natural gas to hundreds of off-takes distributed across Great Britain [42].

Building on the model developed in [34] and on the National Grid Gas Ten Years Statement (GTYS) report from 2015, the network is modeled as a set of 245 nodes and 269 branches [34, 43]. Furthermore, according to the methodology developed in [34], 60 virtual branches are introduced to estimate the network steady-state (see [34] for details).

To spatially embed the NGN within the territory of Great Britain (GB), we adopt the official GIS dataset. The network branches and nodes can be seen in Figure 1. Compared to previous studies on the GB NGN where a simplified

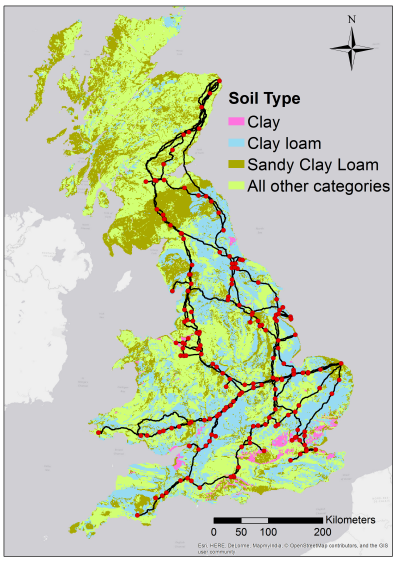

Figure 1: NGN embedded in the Great Britain soil type map; the red dots correspond to the 245 network nodes identified through the GTYS.

network version has been adopted, e.g. [34, 44, 45], our model has a higher spatial resolution, number of components, level of detail and complexity, owing to the use of the GIS dataset.

The GB NGN is managed by five utilities located in different geographic regions, as indicated in Figure 2.

6.1.1. Failure Likelihood

The failure likelihood of every pipe is estimated according to the the procedure described in Section 3.

Failure Probability by External Corrosion. To estimate the failure probability by external corrosion, P_E, we identify the soil type in which pipelines are buried by using the dataset of the British Geological Survey [46]. From this GIS dataset, several soil type categories are merged to fit into the categories reported in Section 3.1 and in [22, 24], i.e. clay, clay loam and sandy clay loam. Soil types that are not assigned to any of these categories are marked as "Other" in Table 1 ([22, 24]).

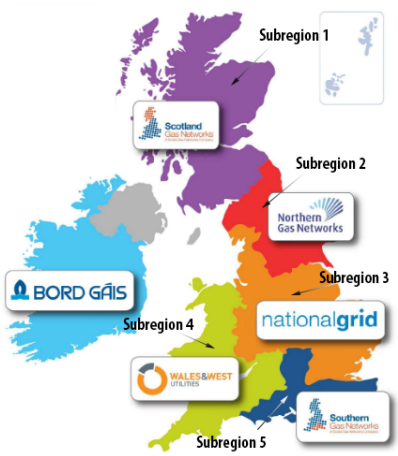

Figure 2: Overview of the 5 utilities managing the NGN in Great Britain [47].

The intersection of the network topology with the soil GIS dataset is performed via the *Intersect* tool in ArcMap, and leads to the identification of 2730 pipeline segments. Figure 1 shows how the four soil categories are distributed in Great Britain. The Monte Carlo procedure described in Section 3.1 is applied to quantify the failure probability due to external corrosion for these 2730 pipeline segments.

Figure 3 shows the mean, the 90-th and the 10-th percentiles of the estimated failure probability for external corrosion as a function of time, for a pipeline segment in a clay loam soil with diameter of 900 mm and average pressure of 77 bar. If no maintenance action is performed, the failure probability due to external corrosion becomes larger than 10^{-5} after roughly 20 years of pipeline operations. Afterwards, external corrosion becomes progressively critical, and its failure probability increases by two orders of magnitude within two decades, i.e. between 20 and 40 years after pipeline installation.

Failure Probability by Internal Corrosion. The approach reported in Section 3.2 is used to estimate the failure probability by internal corrosion, P_I, for the 2730 pipeline segments. Similarly to external corrosion, we account for the uncertainty in the failure probability by internal corrosion by considering the

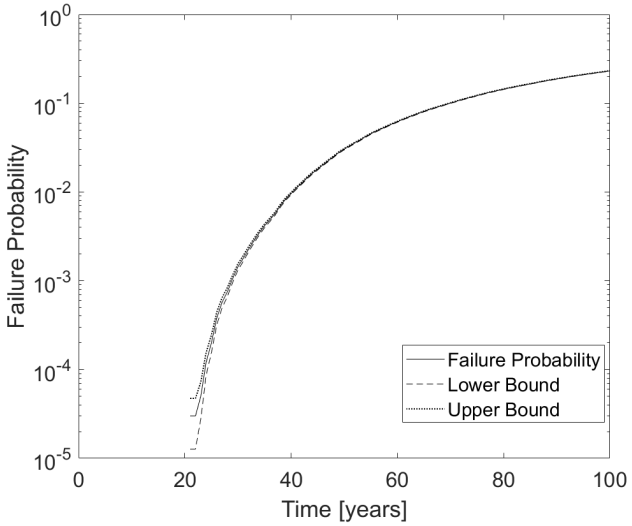

Figure 3: Mean, 90-th and 10-th percentiles of the estimated pipeline failure probability by external corrosion for a sample pipeline (in a clay loam soil with diameter of 900 mm and average pressure of 77 bar) as a function of time. The failure probability is the result of Monte Carlo simulations where the soil properties are randomly sampled from the corresponding distributions in Table 1 and the defect growth in time is modeled using Eq. 1.

80% confidence interval on the MC estimation.

Figure 4 shows the mean, the 90-th and the 10-th percentile of $P_I(t)$ for a pipeline segment with diameter $D = 450$ mm and average pressure of $p = 78$ bar. The failure by internal corrosion becomes larger than 10^{-5} after roughly 10 years of pipeline operations. Afterwards, internal corrosion becomes progressively critical, and its failure probability increases by three orders of magnitude within two decades, i.e. between 10 and 30 years after pipeline installation, if no maintenance action is performed. From the comparison of Figures 3 and 4, we notice that internal corrosion proves to grow remarkably quicker than external corrosion, resulting in a bigger threat to pipeline integrity.

Failure Probability by Third Party Actions. Following the approach described in Section 3.3, the failure probability by third party actions P_{TP} is estimated according to Eq. 8.

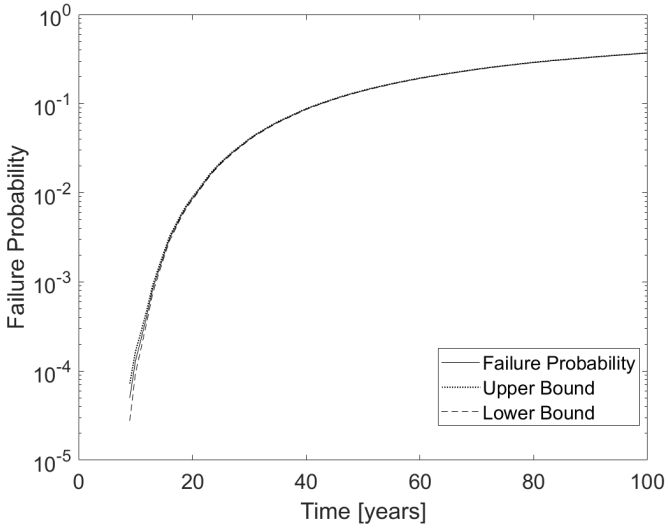

Figure 4: Pipeline failure probability by internal corrosion along the years for a sample pipeline (diameter of 450 mm and average pressure of 78 bar). The failure probability is the result of a Monte Carlo simulation where the natural gas properties are randomly sampled from the corresponding distributions in Table 4 and the defect growth is modeled in time using Eq. 6.

The pipeline diameter is known for each section. Therefore, $\lambda(D)$ values are taken from the latest EGIG publication for each pipe diameter [29, 48]: parameter a_l can be estimated from the data of the EU project CORINE, which provides a high-resolution land-cover data for Great Britain [49]. From the several land-cover categories in [49], only three are considered, i.e. urban, suburban and rural (Figure 5).

Parameters a_c, a_w, and a_p are not known and, thus, they are conservatively set to the largest values of Table 5.

The intersection of the entire NGN with the soil dataset and the land-use dataset results in the identification of 13296 pipeline segments, whose lengths span the orders of magnitude of $10^1 - 10^3$ m. These are reasonable lengths to set a maintenance plan. Therefore, we associate a maintenance project to each pipeline segment, and, thus, the maintenance candidate projects set X contains 13296 projects.

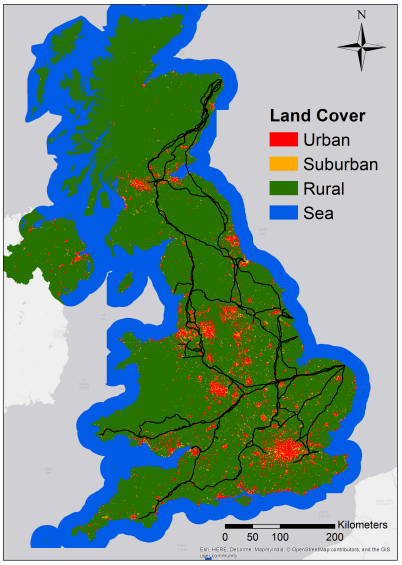

Figure 5: NGN of GB spatially embedded with the CORINE land-cover dataset; the land cover categories are collapsed within the three macro-categories of Table 5 to infer the pipeline failure probability by third party actions [49].

6.1.2. Failure Severity

Hazards to People. To assess the hazard distances according to the jet-fire, fireball and flash fire phenomena, we use the approaches described in Section 4.1.

The hazard distances δ_j^i surrounding each of the previously determined $|X| = 13296$ pipeline segments $i \in X$ for each fire phenomenon $j \in \{jf, fb, ff\}$ are identified by using the *Buffer* tool in ArcMap. Figure 6 shows an example of the overlapped hazard areas determined using this tool for a subset of network pipelines. The resulting hazard distances range in the order of magnitude of $10^1 - 10^3$ m, which are consistent with previous studies performed on similar networks [30, 32] and with historical data, e.g. the Appomatox pipeline failure accident reported in [50].

Finally, the amounts of potentially injured people for each of the three fire phenomena are estimated through Eq. 9 in Section 5 [30, 32].

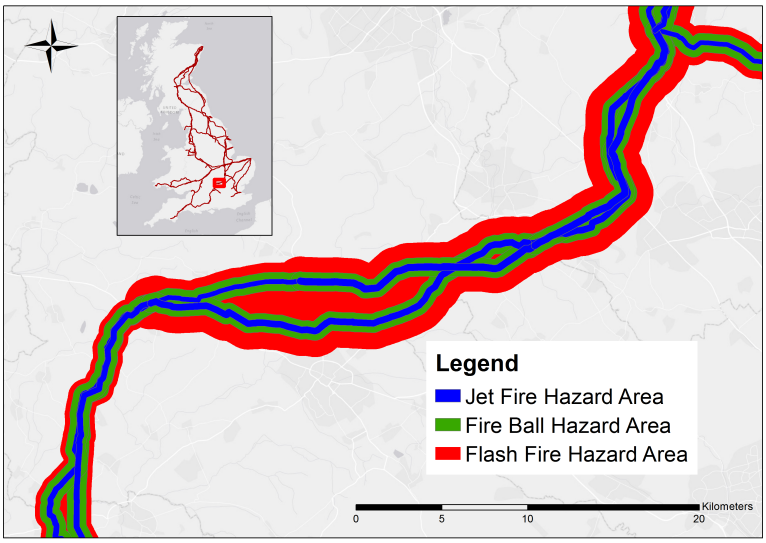

Figure 6: Jet fire, fireball and flash fire hazard distances identified using empirical formulas and Gaussian plume model in Section 4 for a subset of the networks pipelines.

Consequences on Network Operations. The impact of a pipeline failure on the network stability is assessed through the procedure described in Section 4.2. Figure 7 shows the DNS for each network pipeline segment sorted in descending order. Remarkably, the loss of most of the pipeline segments does not lead to network instabilities because of the redundancies in the network connectivity. Nevertheless, approximately 25% of the pipeline segments perform functions that are critical to network operations, and, therefore, their failures create pressure instabilities that can be mitigated only by performing large curtailments of the gas load.

6.2. Pipeline Age Uncertainty and Failure Risk Calculations

The knowledge of the time of pipeline installation is lacking and, therefore, failure probabilities cannot be evaluated deterministically. To represent the corresponding uncertainty, we assign to each pipeline segment an age interval ranging between 0 (brand new pipeline) and 40 years. This assumption on complete uncertainty about the installation time of the pipelines can be overcome

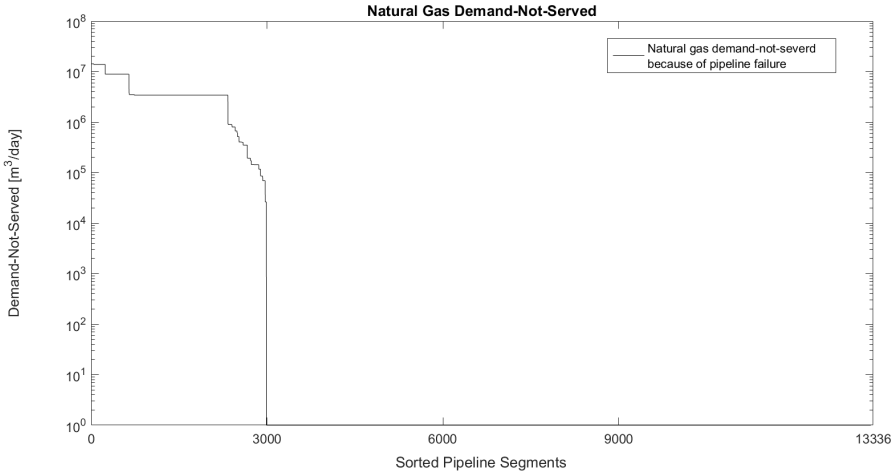

Figure 7: Sorted DNS for the 13296 pipeline segments; some pipeline failures lead to instabilities that can be mitigated only by large gas curtailments.

by using real-life data of the asset, if available.

Figures 8 and 9 show the upper and lower bounds of the failure severity and of the failure probability for the 13296 pipeline segments (or maintenance projects) of the network, respectively, sorted in ascending order. Failure severity and failure probability can vary by several orders of magnitude among the different segments. Moreover, differences of one or two orders of magnitude also occur between the upper and lower bounds for the same pipeline segments. Therefore, the selection of the RBM projects based on failure probability and severity is affected by a significant level of uncertainty and fully justifies the proposed RPM approach.

Finally, with respect to the specific maintenance cost, we assume a minimum value $\underline{c} = 1970£/km \cdot mm$ and a maximum value $\overline{c} = 2290£/km \cdot mm$ [41].

6.3. Results

Following Appendix A, we apply the RPM technique to select the maintenance portfolios in the GB NGN using the three objectives quantified in Section 6, i.e. failure likelihood, severity and project maintenance cost. The weights

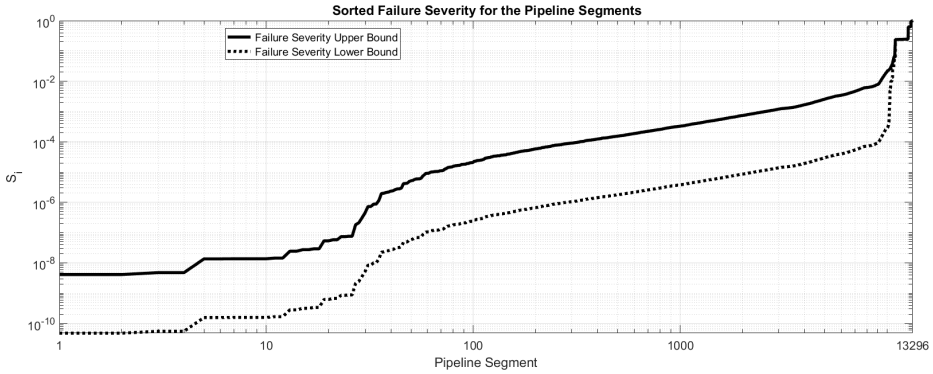

Figure 8: Sorted normalized upper and lower bounds of the failure severity for all the pipeline segments of the network.

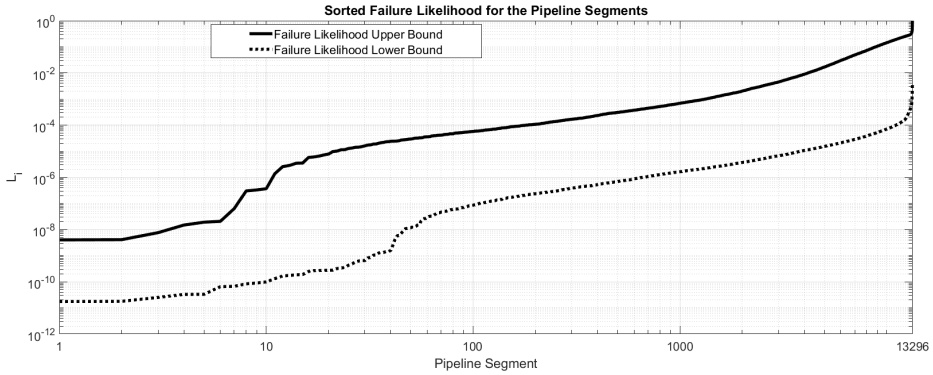

Figure 9: Sorted normalized upper and lower bounds of the failure likelihood for all the pipeline segments of the network.

assigned to the optimization objectives of the multi-criteria project portfolio selection (see Appendix A) are assumed to have no restrictions, i.e. they can freely range between 0 and 1, under the constraint that their sum is equal to 1. This selection allows spanning the entire Pareto optimal set and it is in line with previous studies, in which the maintenance cost is included among the optimization objectives [12], and leads to the following three extreme points in the weights information set I_w [1,0,0], [0,1,0] and [0,0,1].

The developed algorithm runs on the 13296 pipe stretches until 5000 non-dominated portfolios are identified. The computations are carried out with the Matlab MILP-solver and take approximately two hours on a Dual-core, 2.2 GHz, 8 GB memory laptop computer.

One of the key concepts of RPM is the notion of the project-specific Core Index (CI), defined as the share of non-dominated portfolios that include the project (see Appendix A). The CI guides the successive interviews with the DM because all core projects can be surely recommended and all exterior projects (i.e., projects included in non-optimal portfolios) can be safely rejected. Indeed, core projects do and exterior projects do not belong, respectively, to all non-dominated portfolios even if additional information were given [11]. Then, efforts to specify additional score information can be focused on the remaining projects, i.e. borderline projects [11]. This information yields narrower score intervals, which assign the borderline projects to either the sets of core projects or the exterior projects, while not affecting the CI of the previously identified core and exterior projects.

Recognizing that it can be difficult to choose from the set of non-dominated portfolios, the choice of the portfolio could be determined according to appropriate decision rules such as the max-min rule (see Appendix A), which recommends the portfolio that yields the highest minimum overall benefit. This rule coincides with the absolute robustness in robust discrete optimization [11]. The results of the decision rules depend on the set of non-dominated portfolios. This emphasizes the importance of finding as many non-dominated portfolios as possible.

To investigate the network risk reduction as a function of the selection of the maintenance projects and their location, we perform a series of 5-years RPM calculations considering (i) a unique budget GBP $B = 760$ M for the whole network and (ii) a common overall budget divided among the 5 network subregions in Figure 2, proportionally to their total lengths.

Each year, a portfolio is selected from the set of non-dominated portfolios identified by the RPM technique using the $max - min$ criterion as described in Appendix A.

Maintenance actions, i.e. projects, on a pipeline segment, consist in its complete replacement, which resets the pipeline segment age to 0 and decreases the failure probability to its minimum value. To evaluate a summary metric of the overall network risk, we consider the indicator $R^{net} = \sum_{i=1}^{|X|} \overline{R}_i$, where $\overline{R}_i = \overline{\mathcal{L}_i} \cdot \overline{\mathcal{S}_i}$. This indicator sums on both the updated risk values of the projects in the optimal portfolio, which are smaller than before, and the remaining ones, which are more risky because of the increased age. Figure 10 shows the overall effect on the risk indicator over time of implementing each year the optimal portfolio of maintenance projects. We can see that the risk reduction over the years is less effective if the maintenance budget is constrained to be divided into 5 network subregions, proportionally to the total pipe length insisting on the region, compared to the results obtained if one unique budget for the entire network is considered.

To justify this result, we can consider Figure 11, which reports the optimal budget allocation in each subregion resulting from the RPM calculations performed on the whole network. Horizontal lines mark the constant budget that each area receives in the split-budget case. If spatial limitations are not introduced, maintenance focuses on some subregions more than others, e.g. Area 1 (Scotland) and Area 5 (southernmost part of England) receive strong maintenance during the first two years as compared to the case of constant budget. Conversely, Area 3 is very weakly maintained in the first year, i.e. a small amount of critical projects is identified in Area 3, despite containing the largest number of pipelines.

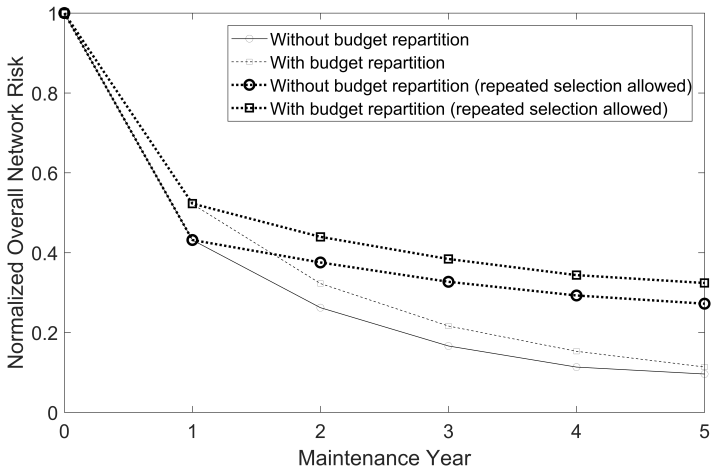

Figure 10: Comparison of the different risk reduction trends for the performed RPM calculations; dashed lines represent the risk trends recorded, if multiple selection along the years of the same maintenance projects is not prevented.

Figure 10 shows two dashed lines corresponding to the risk reduction behavior in case the repeated selection of the same maintenance projects in consecutive years is not prevented. Indeed, in these RPM calculations, maintenance actions only decrease the pipeline segments failure probability but do not affect the other two objective scores, i.e. failure severity and maintenance cost. Consequently, some maintenance projects may be included consistently in the optimum portfolio during multiple years due to their high severity and/or low cost scores. This is because the considered maintenance projects do not include mitigation actions, which decrease the failure severity and prevent the repeated selection of the same project in consecutive years.

Finally, Figure 12 identifies the areas where maintenance actions focus during the first five years of the probability-severity-cost RPM application. In particular, Figure 12 identifies Areas A and D as critical, where maintenance is strongly focused especially during the first two years. The relevance of these areas explains the significant maintenance budget allocated during the first 2 years in Areas 1 and 5 in Figure 11. Similarly, Zones B and C are intensively maintained

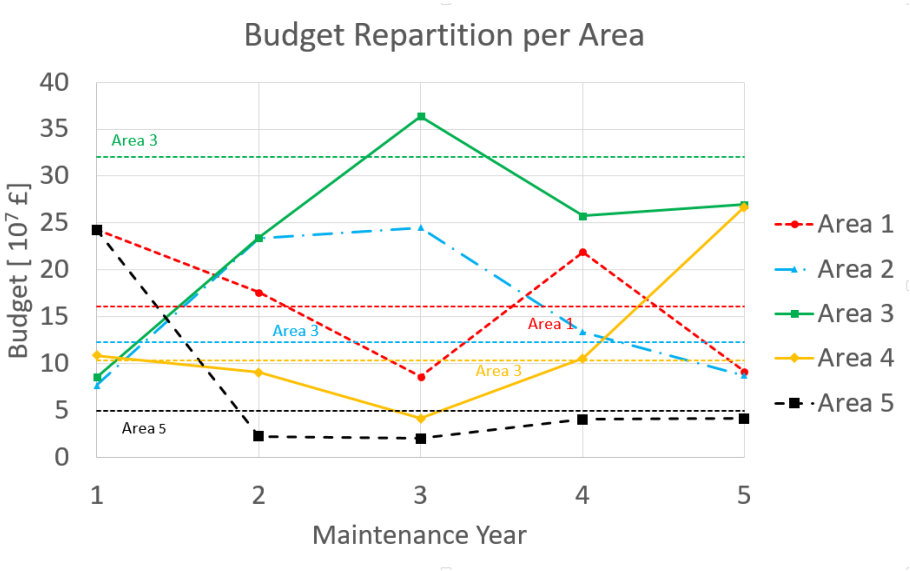

Figure 11: Maintenance budget allocated in each network subregion during the RPM calculations using as objectives failure probability, severity and cost; solid lines: constant budget allocation to each subregion; dashed lines: unique network budget variably allocated to each subregion.

during the first 4 years, even though with a lower intensity compared to Zones A and D. For all the aforementioned areas, criticality is due to the high impact of failures on the network stability. Indeed, all the pipeline segments located there are required to handle very large mass flows up to hundreds of kilograms per hour. Zone E (northernmost, within Area 5) is continuously maintained during the 5 years, but with a lower intensity compared with the aforementioned critical zones. Interestingly, Area 5 is identified as critical also in the previous study on the simplified network described in [16].

7. Discussion: Applicability to Other Contexts

Owing to its generality and modularity, the developed framework can be applied to maintenance planning problems of other NGNs and different types of

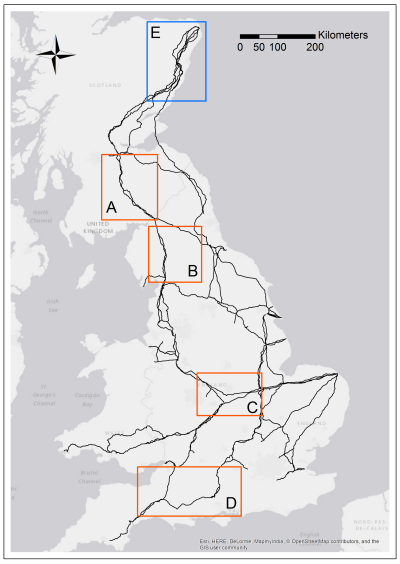

Figure 12: Critical zones where maintenance is focused during the 5 maintenance years presented in Figure 10.

large-scale infrastructures. Indeed, the proposed methodology is made of three general steps, which can be specialized as discussed in the following:

- Identification of the factors defining failure likelihood and severity. These factors depend on both the specific case study and the DMs. Whilst the factors identified and applied in the presented case study can be applied to different NGNs, they need to be re-considered for other types of networks. For example, an more detailed value tree has been proposed for the pipe likelihood in the sewerage system application [14], which considers two levels. The first hierarchical level includes (a) pipe features, (b) past events and (c) local circumstances; the second hierarchical level is further specialized into (a) pipe material, age since last renovation and diameter; (b) number of past blockages and flushing; and (c) soil type and traffic load.

- Assignment of score intervals to every pipe (i.e. project) in the network with respect to each factor of risk severity and likelihood. The methodol-

ogy proposed in this work for NGNs is general: it contains all the theoretical details, it gives the possible values of many model parameters with related uncertainties and it indicates the procedure to identify the data for the application on any NGN (e.g. usage of Corine dataset for land characterization). For the application of the methodology to different contexts, the analysts have to adapt specific solutions for carrying out the "Assignment of score intervals" step. In this respect, the general WING method has been used in [51] to assign an interval of scores to the projects. For every risk factor, the best measurement value (i.e. the one impacting the failure likelihood or severity the most) and the worst one (i.e. the one impacting the failure likelihood or severity the least) are assigned rates 100 and 0, respectively. Then, elicitation questions are posed by first mapping out expert opinions on ordinal preferences for quality differences. Specifically, the expert is asked which 'swing' from a specific attribute value to the best one would result in the largest improvement, the second largest improvement, and so on.

- An optimization algorithm to find the optimal portfolios. In this work, the algorithm proposed in [13] has been adopted, which efficiently identifies a subset of optimal portfolios. Future works will focus on the development of methodologies relying on even more efficient algorithms, as for example the algorithm proposed by Toppila and Salo ([52]).

8. Conclusion

This paper provides a methodology to identify the optimum risk-based maintenance portfolios that can be applied on large networks and, via the RPM technique, handles uncertainties and partial knowledge deficiencies on the objective scores and weights.

The methodology is exemplified with reference to the NGN of Great Britain for a set of multiple years in order to study how maintenance impacts the overall network risk level. The main novelties of the work are:

- Both risk factors are thoroughly characterized through the identification and characterization of their relevant sub-factors. Namely, failure probability is expressed as a combination of three factors corresponding to the three most impacting pipeline failure modes, whereas failure severity is expressed as a combination of two factors, consequences of failures to people and on network operations.

- The GIS data are used to estimate the values of the maintenance plans with respect to some of the identified risk sub-factors. In the case study, the application of a GIS dataset to infer failure probability by third party action and by external corrosion via intersection with the NGN dataset leads to the identification of 13296 pipeline segments, whose lengths range in the order of magnitude of $10^1 - 10^3$ m and which are associated with a corresponding set of 13296 maintenance projects.

- Sequential portfolio selection is considered on an horizon of multiple years, and with different objectives and constraints. RPM application on this case study reveals that if no constraints are introduced on the budget allocation, maintenance actions are focused on some critical zones, e.g. Scotland and the southernmost part of England. Furthermore, the allocation of fixed maintenance budgets to different areas lead to a sub-optimal selection of the maintenance projects and to a less pronounced risk reduction over the maintenance horizon.

Further improvements on the methodology entail introducing synergies and opportunistic cannibalisms on the maintenance projects, e.g. promoting the selection of adjacent pipeline segments. Furthermore, despite local pipeline replacement is the routine maintenance action on a pipeline, other maintenance projects may be introduced, e.g. installing third party actions preventing measures. Finally, the efficiency of the optimization algorithms for identifying the subset of optimal portfolios can also be improved.

References

[1] M.F. Marsaro, M.H. Alencar, A.T. De Almeida, and C.A.V. Cavalcante. Multidimensional risk evaluation: Assigning priorities for actions on a natural gas pipeline. 2014.

[2] T.L. Saaty. *Multicriteria decision making - the analytic hierarchy process. Planning, priority setting, resource allocation.* 1988.

[3] L.M. Candian, L.D.R. Alves, A.G.P. Amorim, and F.D. Pires. Development and prioritization portfolio of natural-gas compression-station projects. 2014.

[4] P.A. Pilavachi, S.D. Stephanidis, V.A. Pappas, and N.H. Afgan. Multi-criteria evaluation of hydrogen and natural gas fuelled power plant technologies. *Applied Thermal Engineering*, 29(11-12):2228–2234, 2009.

[5] A. Jamshidi, A. Yazdani-Chamzini, S.H. Yakhchali, and S. Khaleghi. Developing a new fuzzy inference system for pipeline risk assessment. *Journal of Loss Prevention in the Process Industries*, 26(1):197–208, 2013.

[6] W Kent Muhlbauer. *Pipeline risk management manual: ideas, techniques, and resources.* Gulf Professional Publishing, 2004.

[7] M.J. Gharabagh, H. Asilian, S.B. Mortasavi, A. Zarringhalam Mogaddam, E. Hajizadeh, and A. Khavanin. Comprehensive risk assessment and management of petrochemical feed and product transportation pipelines. *Journal of Loss Prevention in the Process Industries*, 22(4):533 – 539, 2009.

[8] A. Shahriar, R. Sadiq, and S. Tesfamariam. Risk analysis for oil & gas pipelines: A sustainability assessment approach using fuzzy based bow-tie analysis. *Journal of Loss Prevention in the Process Industries*, 25(3):505 – 523, 2012.

[9] P.K. Dey. A risk-based model for inspection and maintenance of cross-country petroleum pipeline. *Journal of Quality in Maintenance Engineering*, 7(1):25–41, 2001.

[10] A.H. Alinia Kashani and R. Molaei. Techno-economical and environmental optimization of natural gas network operation. *Chemical Engineering Research and Design*, 92(11):2106–2122, 2014.

[11] J. Liesiö, P. Mild, and A. Salo. Preference programming for robust portfolio modeling and project selection. *European Journal of Operational Research*, 181(3):1488–1505, 2007.

[12] J. Liesiö, P. Mild, and A. Salo. Robust portfolio modeling with incomplete cost information and project interdependencies. *European Journal of Operational Research*, 190(3):679–695, 2008.

[13] P. Mild, J. Liesiö, and A. Salo. Selecting infrastructure maintenance projects with robust portfolio modeling. *Decision Support Systems*, 77:21–30, 2015.

[14] A. Mancuso, M. Compare, A. Salo, E. Zio, and T. Laakso. Risk-based optimization of pipe inspections in large underground networks with imprecise information. *Reliability Engineering and System Safety*, 152:228–238, 2016.

[15] P.K. Dey, S.O. Ogunlana, and S. Naksuksakul. Risk-based maintenance model for offshore oil and gas pipelines: A case study. *Journal of Quality in Maintenance Engineering*, 10(3):169–183, 2004.

[16] T. Sacco, M. Compare, G. Sansavini, and E. Zio. Robust Portfolio Modelling methodological approach to GB gas grid risk analysis via a simplified network version. 2016.

[17] William transco central penn line south - a citizen's guide. `http://www.lancasterpipeline.org`. Accessed: 2016-05-31.

[18] F.A.V. Bazán and A.T. Beck. Stochastic process corrosion growth models for pipeline reliability. *Corrosion Science*, 74:50–58, 2013.

[19] P. Pedeferri. *Corrosione e protezione dei materiali metallici*. Number v. 2 in Corrosione e protezione dei materiali metallici. Polipress, 2010.

[20] M. D. Pandey, X. X. Yuan, and J. M. van Noortwijk. The influence of temporal uncertainty of deterioration on life-cycle management of structures. *Structure and Infrastructure Engineering*, 5(2):145–156, 2009.

[21] M. Romanoff. *Underground corrosion*. Circular 579. U.S. Govt. Print. Off., 1957.

[22] J.C. Velàzquez, F. Caleyo, A. Valor, and J.M. Hallen. Predictive model for pitting corrosion in buried oil and gas pipelines. *Corrosion*, 65(5):332–342, 2009.

[23] O. Shabarchin and S. Tesfamariam. Internal corrosion hazard assessment of oil & gas pipelines using bayesian belief network model. *Journal of Loss Prevention in the Process Industries*, 40:479–495, 2016.

[24] F. Caleyo, J.C. Velàzquez, A. Valor, and J.M. Hallen. Probability distribution of pitting corrosion depth and rate in underground pipelines: A monte carlo study. *Corrosion Science*, 51(9):1925–1934, 2009.

[25] W. Zhou. System reliability of corroding pipelines. *International Journal of Pressure Vessels and Piping*, 87(10):587–595, 2010.

[26] A. Kale, B.H. Thacker, N. Sridhar, and C.J. Waldhart. A probabilistic model for internal corrosion of gas pipelines. In *2004 International Pipeline Conference*, pages 2437–2445. American Society of Mechanical Engineers, 2004.

[27] W. Liang, J. Hu, L. Zhang, C. Guo, and W. Lin. Assessing and classifying risk of pipeline third-party interference based on fault tree and SOM. *Engineering Applications of Artificial Intelligence*, 25(3):594 – 608, 2012.

[28] X. Wang. *Study on Safety Assessment of City Gas Pipelines*, chapter 184, pages 1749–1760. International Conference on Pipelines and Trenchless Technology 2011, 2011.

[29] WS Atkins Consultants Ltd. An assessment of measures in use for gas pipelines to mitigate against damage caused by third party activity, 2001.

[30] C. Vianello and G. Maschio. Quantitative risk assessment of the italian gas distribution network. *Journal of Loss Prevention in the Process Industries*, 32(1):5–17, 2014.

[31] TNO. *Methods for the determinantion of possible damage to people and objects resulting from the release of hazardous materials - 'Green Book'*. Directorate General of Labour, Notreported, third edition edition, 1992.

[32] C. Vianello and G. Maschio. Risk analysis of natural gas pipeline: Case study of a generic pipeline. *Chemical Engineering Transactions*, 24:1309–1314, 2011.

[33] OGP. Risk Assessment Data Directory, Report No. 434-7; Consequence Modelling, March 2010.

[34] A. Antenucci, B. Li, and G. Sansavini. Impact of power-to-gas on cascading failures in interdependent electric and gas networks. *Lecture Notes in Computer Science (including subseries Lecture Notes in Artificial Intelligence and Lecture Notes in Bioinformatics)*, 9424:36–48, 2015.

[35] A. Osiadacz. *Simulation and analysis of gas networks*. Gulf Publishing Company, Houston, TX, 1987.

[36] R.W. Prugh. Quantitative evaluation of fireball hazards. *Process Safety Progress*, 13(2):83–91, 1994.

[37] P. Melli and E. Runca. Gaussian plume model parameters for ground-level and elevated sources derived from the atmospheric diffusion equation in a neutral case. *Journal of Applied Meteorology*, 18(9):1216–1221, 1979.

[38] Gaussian plume model. `https://personalpages.manchester.ac.uk/staff/paul.connolly/teaching/practicals/gaussian_plume_modelling.html`.

[39] E. Zio. *An Introduction to the Basics of Reliability and Risk Analysis*. World Scientific Publishing Company, 2007.

[40] Natgas.info - the independent natural gas information site. `http://natgas.info/gas-information/what-is-natural-gas/gas-pipelines/`. Accessed: 2016-07-07.

[41] Research Institute. The shale revolution. Technical report, Credit Suisse, December 2012.

[42] National Grid website - United Kingdom. `http://www2.nationalgrid.com/uk/`. Accessed: 2016-07-05.

[43] National Grid. Gas ten years statement - 2015, November 2015.

[44] M. Chaudry, J. Wu, and N. Jenkins. A sequential monte carlo model of the combined gb gas and electricity network. *Energy Policy*, 62:473–483, 2013.

[45] M. Qadrdan, M. Chaudry, J. Wu, N. Jenkins, and J. Ekanayake. Impact of a large penetration of wind generation on the gb gas network. *Energy Policy*, 38(10):5684–5695, 2010.

[46] Soil parent material - british geological survey. `http://http://www.bgs.ac.uk/products/onshore/soilPMM.html/`. Accessed: 2016-06-29.

[47] National Grid website - United Kingdom. `http://www2.nationalgrid.com/uk/`. Accessed: 2016-07-05.

[48] EGIG. 9th Report of the European Gas Pipeline Incident Data Group (period 1970-2013), February 2015.

[49] European Enviroment Agency - CORINE land cover. `http://www.eea.europa.eu/publications/COR0-landcover`. Accessed: 2016-06-05.

[50] William Transco Central Penn Line South - A citizen's guide. `http://www.lancasterpipeline.org`. Accessed: 2016-05-31.

[51] D. Von Winterfeldt. and W. Edwards. *Decision analysis and behavioral research*. Cambridge University Press, 1986.

[52] A. Toppila and A. Salo. Binary decision diagrams for generating and storing non-dominated project portfolios with interval-valued project scores. *European Journal of Operational Research*, 260(1):505 – 523, 2016.

[53] K. Golabi, C.W. Kirkwood, and A. Sicherman. Selecting a portfolio of solar energy projects using multiattribute preference theory. *Management Science*, 27(2):174–189, 1981.

[54] C.E. Kleinmuntz and D.N. Kleinmuntz. A strategic approach to allocating capital in healthcare organizations. *Healthcare Financial Management*, 53(4):52–X5, 1999.

Appendix A. Multi-Criteria Project Portfolio Selection

Let X be a set containing m projects x^j. Given a set of constraints A for feasible portfolios, multi-criteria weighting models are routine approaches to identify the best maintenance projects portfolio p of projects $x^j \in X$ evaluated according to a set I_v^0 of n criteria v weighted according to set I_w^0 of weights w [11, 12]. Among the several feasible portfolios, many authors, e.g. [53, 54], recommend the selection of the portfolio with the highest sum of the overall weighted values of the individual projects, briefly called *portfolio overall value* $V(p, v, w)$, mathematically defined as:

$$V(p, w, v) = \sum_{x^j \in p} V(x^j) = \sum_{x^j \in p} \sum_{i=1}^{n} w_i v_i^j \tag{A.1}$$

Where portfolio p satisfies all the feasibility constraints, i.e. the set of inequalities described as follows:

$$\sum_{x^j \in p} C(x^j) \leq A \tag{A.2}$$

Where C is the feasibility coefficients matrix.

The portfolio selection criterion suggesting to choose the project portfolio having the highest overall value $V(p, v, w)$ cannot be applied if part of the information set, i.e. the objectives scores and the weights assigned to each objective, is not precisely known. In fact, uncertainties on objectives scores v and weights w lead to uncertainties also on the portfolio overall value $V(p, v, w)$. To handle uncertainties and knowledge deficiencies avoiding ventured assumptions, the problem aim shifts from the selection of the highest overall value portfolio to the identification of the non-dominated portfolios set [11, 12, 13].

According to [11], a portfolio p dominates another portfolio p' in the incomplete information set I, defined as the Cartesian product of the incomplete objects scores set I_v and of the incomplete weights set I_w, if:

$$\begin{aligned} &V(p, w, v) \geq V(p', w, v)\ \forall (w, v) \in I \\ &\exists (w, v) \in I | V(p, w, v) > V(p', w, v) \end{aligned} \tag{A.3}$$

If more than a few hundreds projects are involved, the non-deterministic methodology developed in [13] can be applied.

The set of identified non-dominated portfolios is usually called P_N. Every project x^j is assigned a Core Index

$$CI(x^j) = \left|\left\{p \in P_N | x^j \in p\right\}\right| / |P_N| \tag{A.4}$$

On this basis we define the sets of core projects, X_C, exterior projects, X_E, and borderline projects, X_B

$$\begin{aligned} X_C &= \left\{x^j \in X | CI(x^j) = 1\right\} \\ X_E &= \left\{x^j \in X | CI(x^j) = 0\right\} \\ X_B &= \left\{x^j \in X | 0 < CI(x^j) < 1\right\} \end{aligned} \tag{A.5}$$

To select one portfolio p among the several non-dominated portfolios in P_N, several selection criteria have been developed. In this study, we used the $min - max$ criterion, chosen because of the simplicity and clarity of its concept. The $min - max$ criterion suggests to select the non-dominated portfolio having the highest minimum overall value $V(p, w, \underline{v})$, i.e.:

$$P_{min} = arg \max_{p \in P_N} \min_{w \in S_w} V(p, w, \underline{v}) \tag{A.6}$$

Where $\underline{v}$ is the lower bound for the n criteria v and I_w is the set of feasible weights, a subset of I_w including vectors of weights that satisfy the feasibility constraints.

The interested reader can refer to [13, 14] for a more detailed description of this algorithm.

Appendix B. Parameters of the failure modes for external corrosion

The parameters used in Section 3.1 to identify the failure conditions due to external corrosion are explicitly modeled in the following.

The burst pressure for a pipeline is defined as [25]:

$$r_b = \chi \frac{2\sigma_u t}{D}\left[1 - \frac{d_{max}}{t}\left(1 - exp\left(\frac{-0.157l}{\sqrt{\frac{D(t-d_{max})}{2}}}\right)\right)\right] \tag{B.1}$$

Where χ is a multiplicative error term, σ_u is the ultimate tensile strength, d_{max} is the maximum defect depth, l is the defect length in the longitudinal direction, D is the pipe diameter and t is the pipe wall thickness.

The rupture pressure of a pipeline is defined as [25]:

$$r_{rp} = \frac{2t\sigma_f}{MD} \tag{B.2}$$

Where σ_f is the flow stress, defined as $\sigma_f = 0.9\sigma_u$, and M is the Folias factor, defined as follows:

$$M = \begin{cases} \sqrt{1 + 0.6275\frac{l^2}{Dt} - 0.003375\frac{l^4}{D^2t^4}} & \frac{l^2}{Dt} \leq 50 \\ 0.032\frac{l^2}{Dt} + 3.293 & \frac{l^2}{Dt} \leq 50 \end{cases} \tag{B.3}$$